Available online at www.sciencedirect.com

ScienceDirect

www.elsevier.com/locate/jes

JES JOURNAL OF ENVIRONMENTAL SCIENCES

www.jesc.ac.cn

Algal toxicity induced by effluents from textile-dyeing wastewater treatment plants

Hualing Cai [1], *Jieying Liang* [1,2], *Xun-an Ning* [1,3,*], *Xiaojun Lai* [1], *Yang Li* [1]

[1] *School of Environmental Science and Engineering, Guangdong University of Technology, Guangzhou 510006, China*
[2] *School of Chemical Engineering, The University of New South Wales, Sydney, NSW 2052, Australia*
[3] *Guangdong Key Laboratory of Environmental Catalysis and Health Risk Control, Institute of Environmental Health and Pollution Control, Guangdong University of Technology, Guangzhou 510006, China*

ARTICLE INFO

Article history:
Received 31 December 2019
Received in revised form
13 January 2020
Accepted 14 January 2020
Available online 28 January 2020

Keywords:
Textile-dyeing effluent
Ecotoxicity
Alga
Dissolved organic matter
Lipid peroxidation
Metabolic activation

ABSTRACT

This research aimed to evaluate the alga *Scenedesmus obliquus* toxicity induced by textile-dyeing effluents (TDE). The toxicity indicator of TDE in alga at the physiological (algal growth), biochemical (chlorophyll-*a* (Chl-*a*) synthesis and superoxide dismutase (SOD) activity) and structural (cell membrane integrity) level were investigated. Then we further study the relationship among toxicity indicators at physiological and biochemical level, and supplemented by research on algal biomacromolecules. According to the analysis of various endpoints of the alga, the general sensitivity sequence of toxicity endpoints of *Scenedesmus obliquus* was: SOD activity > Chl-a synthesis > algal growth. The stimulation rate of SOD activity increased from day 3 (57.25%~83.02%) to day 6 (57.25%~103.81%), and then decreased on day 15 (−4.23%~-32.96%), which indicated that the antioxidant balance system of the algal cells was destroyed. The rate of Chl-a synthesis inhibition increased gradually, reaching 19.70%~79.39% on day 15, while the rate of growth inhibition increased from day 3 (−12.90% ~10.16%) to day 15 (−21.27%~72.46%). Moreover, the algal growth inhibition rate was positively correlated with the inhibition rate of SOD activity or Chl-*a* synthesis, with the correlation coefficients were 0.6713 and 0.5217, respectively. Algal cells would be stimulating to produce excessive reactive oxygen species, which would cause peroxidation in the cells, thereby destroying chloroplasts, inhibiting chlorophyll synthesis and reducing photosynthesis. With increasing exposure time, irreversible damage to algae can lead to death. This study is expected to enhance our understanding of the ecological risks through algal tests caused by TDE.

Introduction

In recent years, textile-dyeing effluents (TDE) have attracted increasing public attention due to their serious ecotoxicity in the receiving aquatic bodies. In China, about 1.84 billion tons TDE was produced according to the China Environment Statistics Yearbook (2015), mainly in Zhejiang, Jiangsu, and Guangdong provinces. Wastewater discharged from the textile-dyeing industry is a heterogeneous and complex

* *Corresponding author.*
E-mail address: ningxunan666@126.com (X.-a. Ning).
https://doi.org/10.1016/j.jes.2020.01.004

mixture of various pollutants, containing large amounts of dyes, disinfectants, surfactants and other recalcitrant organic substances (Punzi et al., 2015; Liang et al., 2017; Pazdzior et al., 2017). Nearly 85% of organic pollutants in wastewater can be removed after purification via physical, chemical, biological, and other modern treatment processes; however, many degradation products, metabolites, and refractory contaminants with low content but high toxicity still remained after various treatment, which pose serious adverse effects to natural water bodies (Asghar et al., 2015; Zhang et al., 2015; Liang et al., 2018b).

China has formulated a series of wastewater discharge standards to control the adverse effects caused by effluents to the aquatic environment, however, these standards only specify a single physicochemical parameters (such as Chemical Oxygen Demand (COD), Total Phosphorus (TP), Total Nitrogen (TN)) limits. Studies (Bilińska et al., 2016; Balabanic et al., 2017; Yadav et al., 2019) have shown that even if the physicochemical parameters of effluents meet emission standards, they can cause acute, chronic or genotoxic effects on aquatic organisms, which may ultimately pose a threat to aquatic ecosystems. For example, Tigini et al. (2011) reported that the alga *Pseudokirchneriella subcapitata* was the most sensitive to simulated textile wastewater, with a toxic unit (TU) ranging from 3.2 to 45.5. In our previous study (Liang et al., 2018a), we also found that effluents from textile-dyeing treatments plants (TDP) were toxic to various indicator organisms (TU_{50} for *Vibrio fischeri* were 3.56–58.82; TU_{50} for *Desmodesmus subspicatus* were 28.57–71.43), indicating a certain amount of toxicity remained in the discharged effluent. Therefore, the comprehensive impact of wastewater on aquatic ecosystems was not efficient by physicochemical indicators, and biological toxicity monitoring can effectively compensate for this deficiency. The toxicity levels of various wastewaters can be characterized directly through the biological analyses of different organisms, such as algae (Petala et al., 2009; Raptis et al., 2014), which are important primary producers in aquatic ecosystems, fast-growing, easy to grow and any disturbances in their dynamics can affect the balance of the entire ecosystem (Silva et al., 2009). Therefore, *Scenedesmus obliquus (S. obliquus)*, which can be cultivated easily and provides highly reproducible results, was used as a test organism in our toxicity experiments (Yu et al., 2014). Biotoxicity tests with algae are used for wastewater toxicity assessment, at the physiological (algal growth (Yu et al., 2014; Fu et al., 2017)), biochemical (superoxide dismutase (SOD) activity and chlorophyll-*a* (Chl-*a*) synthesis (Hazani et al., 2013; Wei et al., 2014)), and structural (cell membrane integrity) level (Wei et al., 2014; Zhang et al., 2015). However, few studies had investigated the relationship between physiological and biochemical level through algal toxicity tests. Our study aims to gain insight into the relationship among them.

Nowadays, many studies have revealed the relationship between ecological toxicity and various organic parameters of the discharged effluents. A positive relationship was found between the total organic carbon (TOC) and toxicity of wastewater in *Daphnia magna* and *Danio rerio* (Deng et al., 2017a). Our previous study also showed that the COD of different TDE was strongly positively correlated to its toxicity in *Vibrio fischeri* or *Desmodesmus subspicatus* (Liang et al., 2018a). Furthermore, TDE contain a large amount of dissolved organic matter (DOM) with aliphatic or aromatic organic compounds and humic substances (Li et al., 2013). DOM may cause chemical stress in aquatic organisms such as alga, directly or indirectly (Steinberg et al., 2006), by inducing and regulating biotransformation enzymes (Andrea et al., 2004) and modulating (mainly inhibiting) the photosynthetic release of oxygen from freshwater primary producers. Under chemical stress, the metabolic balance of intracellular free radicals is disrupted, which is conducive to the production of free radicals. Excessive free radicals can enhance the peroxidation of cell membrane (Aguiar et al., 2016), thereby damaging the cell membrane system and causing death. Most studies on DOM have focused on their adsorption characteristics and reaction characteristics, and their biological toxicity studies are still rare. Moreover, little research revealed how DOM affects changes in aquatic organism biomacromolecules. Usually, two-dimensional correlation spectroscopy (2D-COS) was used to observe the dynamic structural and compositional changes of a molecular system under the stimulation of external interference. The use of 2D-COS for the elaboration of Fourier Transform Infrared Spectroscopy (FTIR) of synthetic mucilages support the evidence concerning the different roles played by carbohydrates proteins and lipids during the aggregation of organic matter and mucilages (Mecozzi et al., 2009a, b). Therefore, the effect of DOM on algae biomacromolecules under adverse environmental conditions were evaluated by FTIR-2D-COS analysis, which simultaneously determines the protein, lipid, and carbohydrate contents of algal cells at different growth stages (Dean et al., 2010; Meng et al., 2014).

In summary, this study aimed to investigate the ecotoxic effects of effluents from the TDPs on the alga *S. obliquus*, to investigated the relationship between physiological and biochemical level through algae biotoxicity tests, and to further study the effects of DOM on biomacromolecules of algae. It hopefully to provide some useful information for controlling ecological risks of industrial discharged wastewater.

1. Materials and methods

1.1. *Effluent sampling*

TDE samples were collected from four typical TDP (TDE1, TDE2, TDE3, and TDE4), located in Dongguan and Guangzhou of the Guangdong province, southeast China. Table 1 lists the basic information of the four TDPs, including the textile materials, the main dyes used, the operating capacity and the wastewater treatment process. They can be divided into two typical wastewater treatment systems: the first system (TDP 1 and 3) was from the primary sedimentation basin to the anaerobic digester and aeration basin, through the biochemical sedimentation basin or membrane bioreactor to the ozone oxidation basin, representing a typical bio-chemical treatment system. The second system (TDP 2 and 4) includes anaerobic digester and aeration basin then to the physicochemical processes (membrane-filtration or sand filtration),

Table 1 – The basic information of these four TDPs.

TDP	Textile material	Main dyes	operating capacity (m^3/day)	Wastewater treatment process
1	Cotton	Mix dyes	12,000	PC-SB-AD-AB-BSB-OZ
2	Cotton	Ionic dye, disperse dye	14,000	PC-AD-AB-MF
3	Chemical fiber	Ionic dye, acid dye	15,000	PC-SB-AD-AB-MB-OZ
4	Cotton	disperse dye	12,000	PC-AD-AB-SB

PC: Primary clarifier; SB: Sedimentation basin; AD: Anaerobic digester; AB: Aeration basin; BSB: Biological sedimentation basin; OZ: Ozone oxidation; SF: Sand-filtration; AB: Aeration basin; MF: Membrane filtration; BAF: Biological aerated-filtration; MB: Membrane bioreactor.

which represents the typical biochemical treatment system. The composite samples were collected separately into a 5 L polyethylene bottle; after sampling, effluents were filtered immediately through a pre-rinsed 0.45 μm cellulose filter and stored at 4°C for subsequent chemical analyses and toxicity tests.

1.2. *Effluent analysis*

The TP (ammonium molybdate spectrophotometry), NH_3–N (Nessler's reagent colourimetric method), TN (Kjeldahl method), and other basic physicochemical parameters of the effluents were determined according to the standard methods (Chinese NEPA, 2002). In addition, a UV-visible spectrophotometer (UV-2600, Shimadzu, Japan) was used for the measurement of UV absorbance over the range of 250–760 nm, while the dissolved organic carbon (DOC) was determined using a TOC-VCPH analyser (Shimadzu, Japan). All fluorescence measurements were performed in a 1 cm quartz cell, using a steady-transient fluorescence spectrometer (FLS1000, Edinburgh, England), at scanning ranges of 220–480 nm for excitation with 5-nm intervals, and 250–550 nm for emission with 2 nm intervals.

These indicators were within the discharge limits decided by the Discharge Standard of Water Pollutants for Dyeing and Finishing of the Textile Industry (GB4287-2012, China) and the detail description as shown in Appendix A text S1.

1.3. *Ecotoxicity testing of TDE*

1.3.1. *Algal culture*

The algal growth inhibition experiment was carried out with *S. obliquus*, obtained from the Institute of Hydrobiology, Chinese Academy of Sciences (Wuhan, China), and the specific experimental scheme was according to the Guideline 201 of the Organization for Economic Co-operation and Development (OECD, 2011). *S. obliquus* was pre-cultured in 1 L triangle bottles containing BG11 medium at 25 ± 1°C, with cool-white fluorescent light with an intensity of 4000 lux and a 12:12 hr light: dark photocycle. The flasks were shaken manually, several times a day, to obtain a homogenous cell distribution. For the toxicity experiments, the alga was exposed to 25%, 50%, 75%, and 100% (V/V) of the effluent diluted with the BG11 medium to obtain a final test solution volume of 250 mL, for 15 days. The number of algal cells in the flask was adjusted to about 10×4 cells/mL after inoculation. In addition, a control check (CK) group, containing only the BG11 medium, was included for each toxicity test. Each test was performed with triplicate.

1.3.2. *Algal growth inhibition test*

The density of *S. obliquus* was determined in two ways: direct cell counting under a microscope (DM6B, Leica, Germany) with a 0.1 mm deep haemocytometer, and through the measurement of the optical density with a spectrophotometer at 687 nm. Algal density during different periods was determined using the regression equation based on cell and optical densities (Fu et al., 2017). Algal growth was calculated using Eq. (1-1) in Appendix A Table S1.

1.3.3. *Chlorophyll-a synthesis*

The Chl-a concentration was determined using the hot ethanol extraction method (Du et al., 2016). For this, the algal biomass was harvested from 5 mL of well-blended cultures, using a 0.45 μm mixed cellulose membrane. The membrane bearing the algal cells was frozen overnight, and subsequently extracted with 8 mL of hot ethanol in a hot water bath for 2 min. After cooling in the dark for 2 hr, the cells were centrifuged (10,000 r/min, 4°C, 5 min), and absorbance of the supernatant was measured at 665 and 750 nm. In addition, 200 μL of 1 mol/L of HCl was added to the supernatant, and absorbance was measured again after 5 min. The Chl-a concentration (mg/L) was calculated using Eq. (1-2) in Appendix A Table S1.

1.3.4. *Superoxide dismutase activity*

As a key antioxidant defence enzyme, SOD plays an important role in normal cell metabolism. The SOD activity was determined using assay kits from the Jiancheng Bioengineering Institute (Nanjing, China), according to the manufacturer's instructions (Deng et al., 2017b). Briefly, the algal samples were centrifuged (10,000 r/min, 4°C, 10 min), the algal pellets were then re-suspended in cold sodium phosphate-buffered saline (PBS) solution (50 mmol/L, pH 7.8), and then disrupted using an ultrasonic cell disruptor (JY99-IIDN, Xinzhi, China) at 750 W for 10 min. The algal pellets were then re-suspended in cold PBS solution, and the homogenate was centrifuged (10,000 r/min, 4°C, 10 min) to obtain the supernatant for the enzyme activity assay. The SOD activity was calculated according to Eq. (1-3) in Appendix A Table S1.

1.3.5. *Algal cell integrity analysis*

In order to assess membrane characteristics of damaged and normal algal cells, fluorescein diacetate (FDA) and propidium iodide (PI) dyes (Sigma-Aldrich, Milan, Italy), at concentrations of 20 and 10 mg/L, respectively, and a final volume of 3 mL, were used to stain the algal re-suspension (Xiao et al., 2011). After staining, the algal cells were observed under a fluorescence microscope (DM6B, Leica, Germany), with a detection bandwidth of 490–510 nm for FDA, and 540–625 nm for PI, and the images were captured.

1.3.6. *Algal macromolecules analysis*

In order to analyse the influence of wastewater on the alga at a molecular level, further investigating the effect of wastewaters with different humus contents on algal macromolecules, FTIR-2D-COS technology was applied. Algal solution (10 mL) was centrifuged and then dehydrated by freeze-drying, following which 2 mg of the algal cell powder was mixed with 100–200 mg of dry potassium bromide (KBr) and moulded with a hand-operated hydraulic press (Atlas, Specac, England). The infrared measurements were recorded using a Fourier transform infrared spectrophotometer (Nicolet 6700, Thermo-Fisher, USA), in the range of 4000-400 cm^{-1} wave number.

1.4. *Statistical analyses*

One-way analysis of variance (ANOVA) was used to test for differences, with a significance level of $p < 0.05$. Spearman correlation analysis was used to study correlations among different toxicity indicators. 2D-COS was performed in 2D-shige (Kwansei-Gakuin University, Japan) to ascertain minor variations in the different spectra resulting from external disturbances. All statistical analyses were conducted using Origin 2018 (Origin Lab, USA) or SPSS 21.0 (IBM, USA).

2. Results and discussion

2.1. *Effect of TDE at physiological level (algal growth)*

As shown in Table 2, the growth stimulation rates in all the experimental groups reached their highest levels on day 6, ranging from 0.19% to 74.35%. In the 25% (V/V) group, the growth inhibition rates of the samples from TDE1-TDE4 on day 6 were −56.70%, −74.35%, −60.97%, and −39.11%, respectively, while the rates on day 15 were 30.72%, −4.73%, 29.51%, and 52.22%, respectively, indicating a stress response in the samples. Appendix A Fig. S2 further shows that the densities of algal cells in all the 25% (V/V) experimental groups were higher than that in the control group. In particular, the cell densities of TDE2 and TDE4 on day 15 were significantly higher than that of the CK group. However, for the 75% and 100% (V/V) groups, the cell density decreased with increasing concentration and time, exhibiting values lower than that of the CK group, and this trend was the most obvious for TDE4. The CK group had a stable growth trend in the last period of exposure (day 6~day 15), while growth in the experimental groups had slowed down, most likely because metabolic activation damaged the algal cells at later exposure stages. This was particularly the case for TDE2 and TDE4 in the 50% (V/V) group. Interestingly, among the algal growth inhibition rates on day 15, the rates of TDE2 and TDE4 were relatively high, ranging from −4.73% to 71.45% and from −9.62% to 74.26%, respectively. These observations prove that the initial induction from metabolic activation, probably caused by the presence of humic substances, compensates for the biological processes that eventually cause disturbance of the internal environmental homeostasis, leading to irreversible damage and a decrease in growth rates (Nestler et al., 2012).

2.2. *Effect of TDE at biochemical level*

2.2.1. *SOD activity*

Appropriate SOD activity can eliminate redundant reactive oxygen species (ROS) and reduce the potential toxicity of pollutants in algae (Deng et al., 2017b). However, excessive

Table 2 – Comparison of the indices of the experimental groups and the CK group (%) on days 3, 6, and 15. The chromaticity graph of red-grey-blue was used to express inhibition rate; a darker blue colour indicates a higher inhibition rate, and a darker red colour indicates a higher stimulation rate (negative inhibition rate). * indicates a statistical difference between the experimental groups and the CK group ($p < 0.05$).

	Algal growth inhibition rate (%)				SOD activity inhibition rate (%)				Chl-a synthesis inhibition rate (%)			
	25%	50%	75%	100%	25%	50%	75%	100%	25%	50%	75%	100%
TDP1~3	-7.75	7.33	7.06	10.16	-62.03*	-70.27*	-83.02*	-81.79*	5.10	-1.22	27.27	20.88
TDP1~6	-56.70*	-52.18*	-15.41	-11.49	-68.97*	-75.93*	-93.38*	-95.72*	21.12	18.73	14.41	65.47*
TDP1~15	30.72	14.04	44.45	42.33	-12.87	-14.41	-10.69	-32.96	19.70	57.56*	60.15*	66.77*
TDP2~3	6.48	1.88	-9.58	3.08	-83.20*	-77.92*	-69.81**	-64.17	9.86	-7.55	17.17	49.45*
TDP2~6	-74.35*	-0.19	-44.52*	-19.30	-81.73*	-82.33*	-81.88*	-83.32*	-11.95	4.77	19.71	68.35*
TDP2~15	-4.73	68.27*	71.45*	21.27	2.69	-5.36	-6.10	-14.44	25.41	48.67*	78.95*	79.39*
TDP3~3	-2.00	1.23	0.43	6.26	-81.33*	-69.35*	-57.25*	-81.6*	-14.51	10.16	33.33*	35.17*
TDP3~6	-60.97*	-33.71*	-54.39*	-8.00	-73.92*	-77.16*	-73.76*	-103.81*	-14.74	-6.76	12.61	46.04*
TDP3~15	29.51	12.19	30.65	9.88	0.71	-2.84	-18.86	-24.43	34.44	35.2	66.67*	69.23*
TDP4~3	-12.9	5.05	-11.59	9.27	-75.76*	-67.80*	-79.7*	-76.31*	-23.37	-1.22	26.26	40.66*
TDP4~6	-39.11*	-58.26*	-46.56*	-38.68*	-77.31*	-72.72*	-77.99*	-91.31*	-9.96	-1.62	22.52	61.15*
TDP4~15	52.22*	5.61	74.26*	9.62	4.23	-0.99	-3.83	-7.7	48.92*	50.83*	79.45*	76.92*

ROS is produced when organisms are stimulated by an external stimulus (such as humic substances), which interferes with the dynamic equilibrium of organisms and results in oxidative stress, leading to toxic effects (Dao and Beardall, 2016). According to Appendix A Fig. S2, the SOD activity was lower in the CK group than in the experimental groups, and it increased gradually with increasing time of exposure. However, as shown in Table 2, the promotion rates of SOD activity in different groups first increased and then decreased over time, with values of 68.97%–103.81% on day 6 and the lowest values on day 15. For TDE2 and TDE4, the promotion rates over 15 days ranged from −2.69% to 14.44% and from −4.23% to 7.70%, respectively. Notably, in the 25% (V/V) experimental groups, the promotion rates of TDE2, TDE3, and TDE4 on day 15 were −2.69%, −0.71%, and −4.23%, respectively, indicating a lower SOD activity compared to that of the CK group. Previous studies (Calabrese et al., 2012; Agathokleous, 2018) have shown that an increase in the antioxidant defence enzymes (such as SOD) occurs in response to metabolic activation; when algae are exposed to different effluents, SOD activity is stimulated due to mild oxidative stress. However, this activity is severely suppressed by increasing oxidative stress over time, resulting in the loss of compensatory quality (Liu et al., 2009). When the content of accumulated ROS exceeds the scavenging ability of intracellular enzymes, lipid peroxidation occurs in the cell membrane, resulting in impaired cell function (Dao and Beardall, 2016). This phenomenon is more distinct at higher levels of humus.

It is evident from these results that SOD plays an important role in normal cell metabolism and in scavenging excess ROS. It is an excellent indicator of TDE toxicity in algae, and the sharp decline in SOD activity is related to the destruction of the algal defence mechanism.

2.2.2. *Chl-a synthesis*

The contents of photosynthetic pigments, such as Chl-*a*, are effective indicators of algal cells growth (Deng et al., 2017b). In the present study, the Chl-*a* content of algal cells in the CK group increased gradually over time, while that in the experimental groups also increased, but to a lower extent (Appendix A Fig. S2). In addition, several experimental groups exhibited a slight decrease in the later stage. For example, in the 75% (V/V) TDE2 experimental group, the Chl-a content decreased from 1.887 to 1.523 mg/L from day 12 to day 15, due to irreversible damages to the cell membrane or to the chlorophyll synthesis capacity (Blokhina et al., 2003), caused by long-term exposure to adverse environmental conditions. Some of our findings are consistent with those of Zhang et al. (2015) who found that the Chl-*a* content of algae exposed to wastewater effluents for 3 days was higher than that of the CK group. In the present study, the Chl-a contents of the 25% (V/V) TDE3 and TDE4 groups were 1.68 and 1.81 mg/L, respectively, which increased by 14.51% and 23.37%, respectively, compared to the CK group. However, Zhang et al. (2015) only studied the Chl-*a* content of algae exposed to wastewater for 3 days, ignoring the accumulated toxicity over time. However, as shown in Table 2, with increasing sample concentration and time of exposure, the inhibition rate of Chl-*a* synthesis gradually increased, especially in TDE2 and TDE4. On day 15, the inhibition rate in TDE2 and TDE4 samples ranged from 25.41% to 79.39% and from 48.92% to 79.45%, respectively. Among the experimental groups, the lowest inhibition rates were found for 25% (V/V) TDE1, with rates of 5.10%, 21.12%, and 19.70% on days 3, 6, and 15, respectively. The highest inhibition rates were found for 100% (V/V) TDE4, ranging from 40.66% on day 3–76.92% on day 15. These results are possibly due to the increasing amount of humus adsorbed to the surface of the algal cells, allowing more pollutants to enter the cells and destroy the chloroplast structure (Elayan et al., 2008; Bahrs and Steinberg, 2012), further inhibiting Chl-*a* synthesis.

In general, the contents of Chl-*a* were significantly different between the experimental and CK groups ($p < 0.05$) over a longer period, indicating that chlorophyll synthesis is extremely sensitive and more susceptible to external influences than the algal growth (Wei et al., 2014). Therefore, the inclusion of Chl-a synthesis in future monitoring projects is highly recommend.

2.3. *Relationship among toxicity indicators at physiological and biochemical level*

In this study, the correlations among toxicity indicators at physiological and biochemical level of alga were investigated. Fig. 1 show the correlation between algal growth inhibition rate and SOD activity or Chl-*a* synthesis inhibition rate through algal toxic test, and the data depicted in Fig. 1 indicated evident correlation ($P < 0.05$). It was found that the algal growth inhibition rate was positively correlated with the inhibition rate of SOD activity or Chl-a synthesis, with the correlation coefficients were $r_1 = 0.6713$ and $r_2 = 0.5217$; and the slopes of lines were 0.658 and 0.482, respectively.

Initially, cell growth and Chl-*a* synthesis were promoted, and the activity of SOD was stimulated. This is because algae can degrade and utilize DOM to a certain extent, transforming them into growth substances that can be utilized by themselves. Weak stimulation can accelerate vitality, which is the hormesis (Calabrese and Blain, 2011). However, negative effects began to appear over time. DOM components themselves are non-toxic or less toxic; but the metabolites formed after their *in vivo* biological transformation are more toxic than the parent substances. It can be intuitively found from Fig. 1a that the range of algal growth inhibition rate was ranged from −80% to 80%, and most of them are concentrated at −20% ~20%. The inhibition rate of SOD activity was mainly jumped from −60%~-80% to −20%~0%. In the experimental group, SOD enzyme can convert the ROS generated by algal into a less active substance in the enzymatic defence system, thereby reducing or eliminating the attack of ROS on the biofilm, and protecting the membrane lipid from excessive oxidation. However, with the increase of the exposure concentration or time (combined with Table 2), the ROS produced by algae are more toxic, which inhibits the activity of SOD, accumulating excessive ROS to damage the algal biofilm (Agathokleous, 2018; Calabrese, 2016) and thus with a higher algal growth inhibition rate. The inhibition rate of Chl-*a* was evenly distributed from −30% to 80% as shown in Fig. 1b. In conjunction with Table 2, both algal growth and Chl-*a* synthesis inhibition rate gradually increases over exposure time. In addition, the increase of the inhibition rate of Chl-*a*

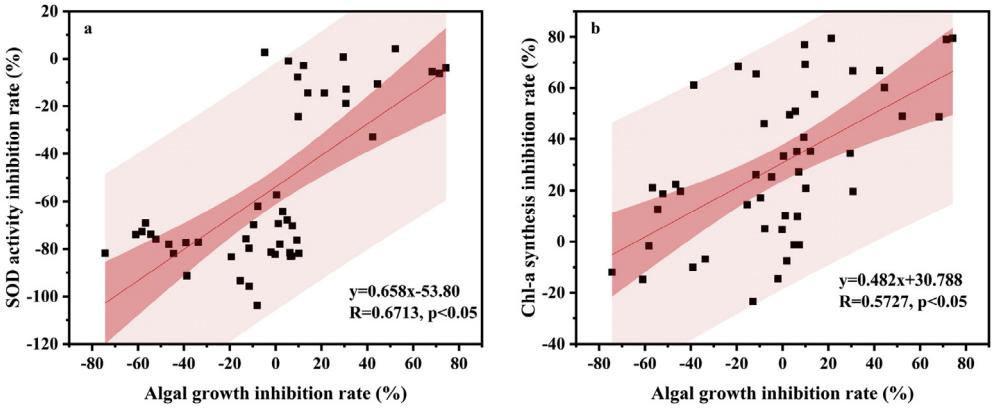

Fig. 1 – Correlation between algal growth inhibition rate and SOD activity inhibition rate (a) or Chl-*a* synthesis inhibition (b) through algal toxic test.

synthesis showed a stable trend, and has a certain buffer period. This possibly due to alga first experienced SOD activity inhibition and biofilm lipid peroxidation, which resulted in the destruction of the chlorophyll structure. In this sense, various membrane structure functions of the synthetic chlorophyll were also reduced, resulting in a decreased Chl-*a* content, subsequently impeding cell growth (Du et al., 2016; Taibi et al., 2016). Thus, the correlation coefficients $r_1 > r_2$. This calls for a more thorough investigation of these factors when evaluating the ecotoxicity of TDE to alga.

2.4. *Effect of TDE at structural level*

2.4.1. *Cell membrane integrity*

Fig. 2a shows the algal cell membrane integrity assessments using stained 25% (*V*/*V*) groups on days 5, 10, and 15. The details of other experimental groups are displayed in Appendix A Fig. S3. Red-stained cells indicate damaged membranes, whereas green-stained cells indicate intact membranes. The algal cell density (Appendix A Fig. S2) and the number of red-stained cells gradually increased with increasing time of exposure. Although the cell density of the CK group was lower, the cells were plump, and most cell membranes were still intact on day 15. In TDE1-4 experimental groups, numerous red-stained cells were found in the second fluorescence staining. Moreover, on day 15, the number of ruptured cells was higher, and the cells were smaller than normal algal cells, especially in TDE2 and TDE4. Fig. 2b illustrates the typical cell morphologies observed using optical microscopy. The normal algal cells (Fig. 2b.A) were fresh green and spindle-shaped with tapered ends, while the affected cells (Fig. 2b.B-D) were dark green, with blurry pigment blobs and unusual shapes, suggesting cell damage. Although the algal cells in the experimental groups displayed higher density over a shorter period of time, most cell membranes were destroyed. From the previous analysis of SOD activity, SOD activity gradually increases at the beginning, and when it reaches a certain concentration, alga will be overcompensated in response to homeostasis, leading to the destruction of cell structure and slowing cell growth in the later stage. Thus, cell density alone cannot be used to evaluate the toxic effects of effluents on algae. Membrane damage can affect cell division and reproduction, thereby inhibiting algal growth. A longer time of exposure is needed for this phenomenon to be observed.

2.4.2. *Algal macromolecules*

To investigating the effect of TDE with different humus contents on algal macromolecules, the most representative samples (TDE1 and TDE4) were selected. The macromolecular modifications in the alga under adverse environmental conditions were evaluated by infrared spectrum analysis, which simultaneously determines the protein, lipid, and carbohydrate contents of algal cells at different growth stages (Dean et al., 2010; Meng et al., 2014).

According to Fig. 3 and Appendix A Tables S3-4, the infrared absorption spectra of the alga in TDE1 and TDE4 groups showed slight changes from day 3 onwards, compared to those of the CK group, i.e., there was a new absorption peak at 2950–2810 cm^{-1}, probably caused by lipids and proteins. Two other protein absorption regions at 1655 cm^{-1} (amide I) and 1548 cm^{-1} (amide II) were observed, reflecting the changes in the secondary structure of proteins. The peak absorption value of vibration, around 1,382 cm^{-1} (potentially caused by lipids, carbohydrates, and proteins), increased in the CK group, but decreased in the experimental groups throughout the exposure period. The 2D-IR COS results were used to determine the functional groups of algal molecules in the 3000–1000 cm^{-1}-region that changed first during stress. Using the sequential order rules (Chen et al., 2015), we concluded that the structural change sequence followed the order $C(CH_3)_2$ symmetric → Amide II → Amide I → CH_2 asymmetric. Previous research (Chen and Jiang, 2011) has shown that the cell membrane was the first site to be attacked, when algae were exposed to adverse environmental conditions; the contaminant disrupted the membrane by altering the water-solubility of the membrane lipid molecules (the absorption peak value in 1382 cm^{-1} decreased). In addition, the ROS stimulated algae to produced proteins with new characteristics (the new absorption peak values at 1548 cm^{-1} increased) and stimulated the accumulation of proteins in the cells (the absorption peak values at 1655 cm^{-1} increased). SOD enzymes can also be activated by mild oxidative stress to

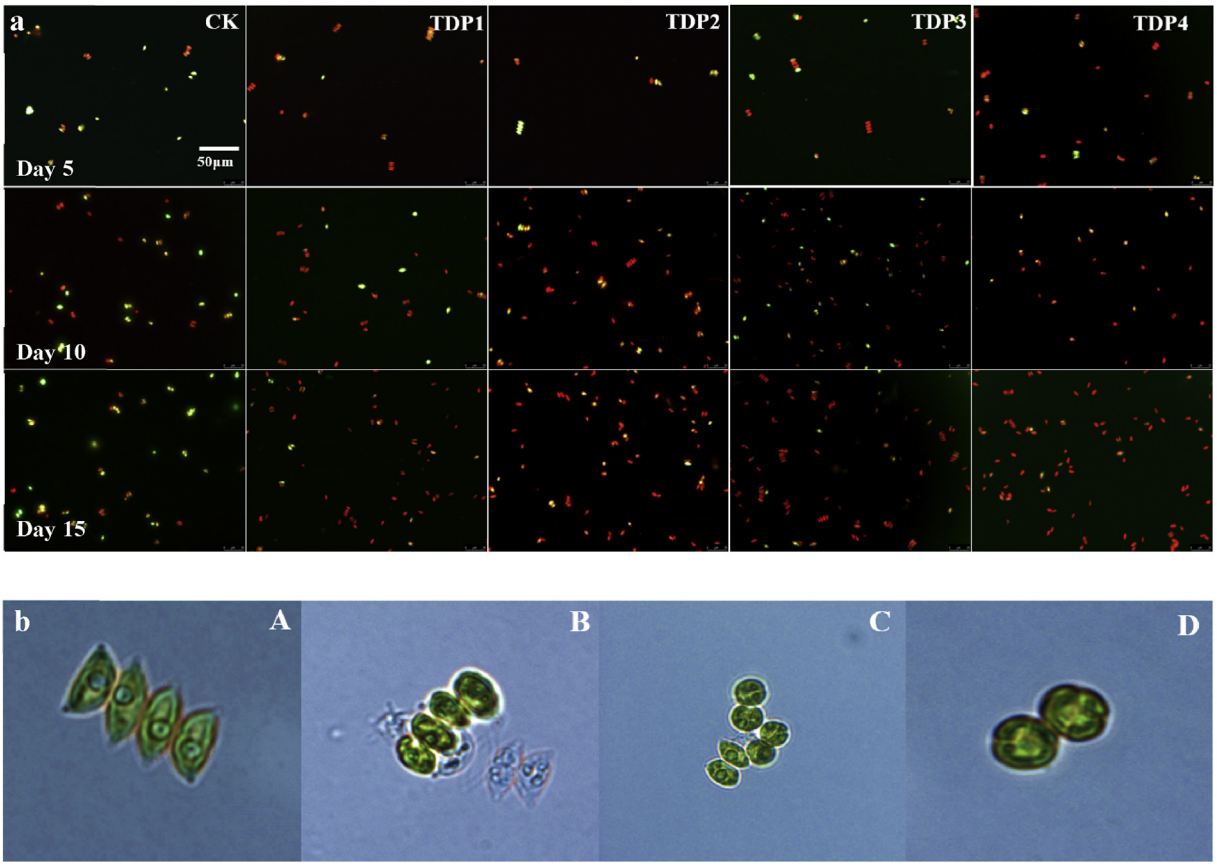

Fig. 2 – Fluorescence microscopic images of *S. obliquus* on days 5, 10, and 15 (from top to bottom) at 25% (V/V) TDE exposure. Red-stained cells indicate damaged membranes, and green-stained cells indicate intact membranes (a). Morphology of algal cells under an optical microscope; A represents normal algal cells; B, C, and D represent typical abnormal algal cells at 25% (V/V) TDE exposure (b).

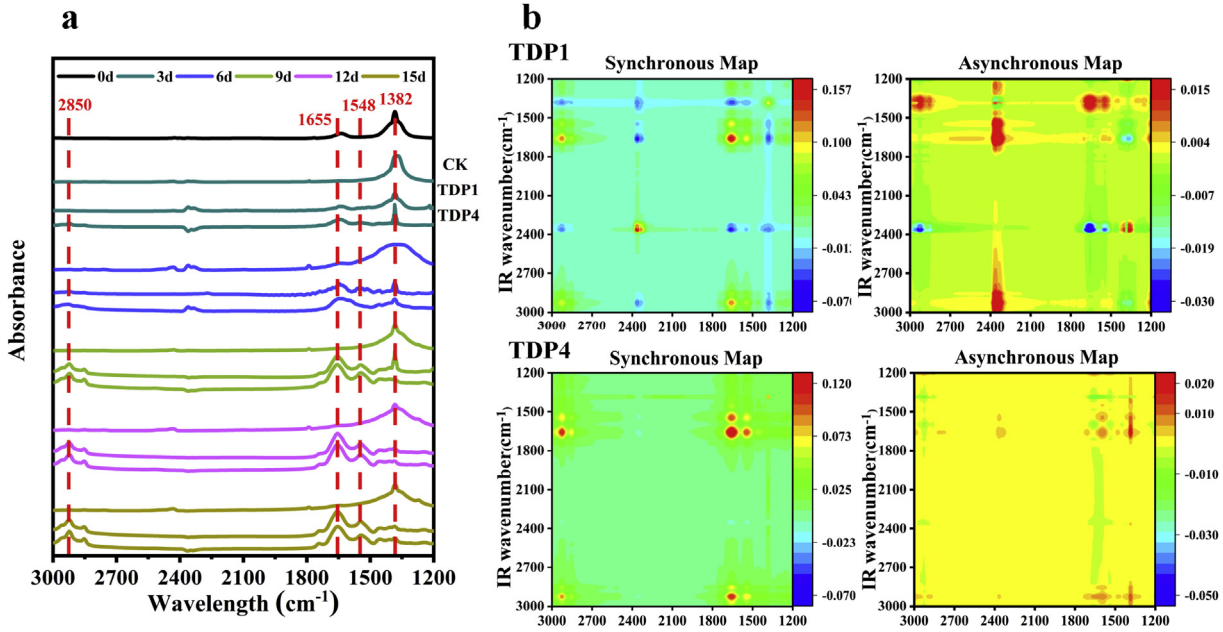

Fig. 3 – FTIR absorption spectra (a) and corresponding 2D-IR correlation maps (b) of the alga throughout the exposure period. The numbers, 0, 3, 6, 9, 12, and 15 refer to the results of the infrared measurements of algal cells recorded on days 0, 3, 6, 9, 12, and 15, respectively.

maintain cell structure and functional stability; however, this activity is seriously inhibited when oxidative stress increases, resulting in the loss of the compensation mechanism (Yang et al., 2014; Ramadass et al., 2017; Ni et al., 2018). Algal cells synthesize fatty acids by regulating lipid metabolism (the absorption peak values at 2850 cm^{-1} increased). Algae can synthesize unsaturated fatty acids to maintain the relative fluidity of the cell membrane under normal conditions (Richardson et al., 2017). Previous studies (Halliwell and Chirico, 1993; Zhang et al., 2018; Zhang et al., 2019) have shown that free radicals, especially ROS, can change the molecular structure of membrane lipids through lipid peroxidation, which manifests as a reduction in C=C in the hydrocarbon chain and the release of free fatty acids. Hydrogen atoms in the olefins adjacent to polyunsaturated fatty acids are the most vulnerable to oxidative attacks, resulting in a reduction of their contents and ultimately in the destruction of the membrane system (Ni et al., 2018).

Based on this, when algal cells are exposed to adverse environmental conditions, they may undergo the following steps: (1) DOM enters the algal cells by occupying channels that transport water and nutrients, thereby affecting the metabolic process. (2) Contaminants are metabolically activated, stimulating algal cells to produce excess ROS, resulting in peroxidation in the cells. Lipids and proteins in the algal cell membrane are the primary targets of the oxidative attacks. Peroxidation of lipid membranes destroys the structure and function of cell membranes (Kramarova et al., 2012). (3) The activity of antioxidant enzymes such as SOD is further inhibited, resulting in an antioxidant imbalance in the cell (Pandey et al., 2012). (4) The chloroplasts are destroyed, chlorophyll synthesis is inhibited, and photosynthesis is reduced (Bahrs and Steinberg, 2012; Neilen et al., 2017). Irreversible damage to the algal cells leads to death as time of exposure increases.

3. Conclusions

The assessment of TDE toxicity could select a comprehensive assessment of the various indicators. Among those endpoints used in our study to characterize the ecotoxicity to *S. obliquus*, the inhibition rate of SOD activity and Chl-*a* synthesis had a high positive correlation with the algal growth inhibition rate of algae. The accumulation of excessive ROS at later stages resulted in lipid peroxidation, which destroyed the cell membrane and chloroplast, leading to cell death. This ecotoxicological approach provides valuable information about the effects of industrial discharges in the receiving waters, and it is suggested that more attention could be paid to the DOM composition and ecotoxicity of textile-dyeing wastewater.

Declaration of competing interest

The authors declare that they have no known competing financial interests or personal relationships that could have appeared to influence the work reported in this paper.

Acknowledgments

This work was supported by the Local Innovative and Research Teams Project of Guangdong Pearl River Talents Program (No. 2017BT01Z032), the Natural Science Foundation of China (No. 21577027), the 2017 Central Special Fund for Soil, Preliminary Study on Harmless Treatment and Comprehensive Utilization of Tailings in Dabao Mountain (No. 18HK0108).

Appendix A. Supplementary data

Supplementary data to this article can be found online at https://doi.org/10.1016/j.jes.2020.01.004.

REFERENCES

Agathokleous, E., 2018. Environmental hormesis, a fundamental non-monotonic biological phenomenon with implications in ecotoxicology and environmental safety. Ecotoxicol. Environ. Saf. 148, 1042–1053.

Aguiar, N.O., Medici, L.O., Olivares, F.L., Dobbss, L.B., Torres-Netto, A., Silva, S.F., et al., 2016. Metabolic profile and antioxidant responses during drought stress recovery in sugarcane treated with humic acids and endophytic diazotrophic bacteria. Ann. Appl. Biol. 168 (2), 203–213.

Andrea, P., Steffen, H., Vogt, R.D., Beate, R.D., Kent, B., Steinberg, C.E.W., 2004. Photogeneration of singlet oxygen by humic substances: comparison of humic substances of aquatic and terrestrial origin. Photochem. Photobiol. Sci. 3 (3), 273–280.

Asghar, A., Raman, A.A.A., Daud, W.M.A.W., 2015. Advanced oxidation processes for in-situ production of hydrogen peroxide/hydroxyl radical for textile wastewater treatment: a review. J. Clean. Prod. 87, 826–838.

Bahrs, H., Steinberg, C.E., 2012. Impact of two different humic substances on selected coccal green algae and cyanobacteria-changes in growth and photosynthetic performance. Environ. Sci. Pollut. Res. Int. 19 (2), 335–346.

Balabanic, D., Filipic, M., Krivograd Klemencic, A., Zegura, B., 2017. Raw and biologically treated paper mill wastewater effluents and the recipient surface waters: cytotoxic and genotoxic activity and the presence of endocrine disrupting compounds. Sci. Total Environ. 574, 78–89.

Bilińska, L., Gmurek, M., Ledakowicz, S., 2016. Comparison between industrial and simulated textile wastewater treatment by AOPs – Biodegradability, toxicity and cost assessment. Chem. Eng. J. 306, 550–559.

Blokhina, O., Virolainen, E., Fagerstedt, K.V., 2003. Antioxidants, oxidative damage and oxygen deprivation stress: a review. Ann. Bot. 91 (2), 179–194.

Calabrese, E.J., 2016. The emergence of the dose-response concept in biology and medicine. Int. J. Mol. Sci. 17 (12).

Calabrese, E.J., Blain, R.B., 2011. The hormesis database: the occurrence of hormetic dose responses in the toxicological literature. Regul. Toxicol. Pharmacol. 61 (1), 73–81.

Calabrese, E.J., Iavicoli, I., Calabrese, V., 2012. Hormesis: why it is important to biogerontologists. Biogerontology 13 (3), 215–235.

Chen, H., Jiang, J.G., 2011. Toxic effects of chemical pesticides (trichlorfon and dimehypo) on Dunaliella salina. Chemosphere 84 (5), 664–670.

Chen, W., Habibul, N., Liu, X.Y., Sheng, G.P., Yu, H.Q., 2015. FTIR and synchronous fluorescence heterospectral two-

dimensional correlation analyses on the binding characteristics of copper onto dissolved organic matter. Environ. Sci. Technol. 49 (4), 2052–2058.
Dao, L.H., Beardall, J., 2016. Effects of lead on growth, photosynthetic characteristics and production of reactive oxygen species of two freshwater green algae. Chemosphere 147, 420–429.
Dean, A.P., Sigee, D.C., Estrada, B., Pittman, J.K., 2010. Using FTIR spectroscopy for rapid determination of lipid accumulation in response to nitrogen limitation in freshwater microalgae. Bioresour. Technol. 101 (12), 4499–4507.
Deng, M., Zhang, Y., Quan, X., Na, C., Chen, S., Liu, W., et al., 2017a. Acute toxicity reduction and toxicity identification in pigment-contaminated wastewater during anaerobic-anoxic-oxic (A/A/O) treatment process. Chemosphere 168, 1285–1292.
Deng, X.Y., Cheng, J., Hu, X.L., Wang, L., Li, D., Gao, K., 2017b. Biological effects of TiO2 and CeO2 nanoparticles on the growth, photosynthetic activity, and cellular components of a marine diatom Phaeodactylum tricornutum. Sci. Total Environ. 575, 87–96.
Du, S., Zhang, P., Zhang, R., Lu, Q., Liu, L., Bao, X., et al., 2016. Reduced graphene oxide induces cytotoxicity and inhibits photosynthetic performance of the green alga *Scenedesmus obliquus*. Chemosphere 164, 499–507.
Elayan, N.M., Treleaven, W.D., Cook, R.L., 2008. Monitoring the effect of three humic acids on a model membrane system using 31P NMR. Environ. Sci. Technol. . 42 (5), 1531–1536.
Fu, L., Huang, T., Wang, S., Wang, X., Su, L., Li, C., et al., 2017. Toxicity of 13 different antibiotics towards freshwater green algae *Pseudokirchneriella subcapitata* and their modes of action. Chemosphere 168, 217–222.
Halliwell, B., Chirico, S., 1993. Lipid peroxidation: its mechanism, measurement, and significance. Am. J. Clin. Nutr. 57 (5 Suppl), 715S–724S discussion 724S-725S.
Hazani, A.A., Ibrahim, M.M., Shehata, A.I., El-Gaaly, G.A., Daoud, M., Fouad, D., et al., 2013. E Ecotoxicity of Ag-nanoparticles on two microalgae, *Chlorella vulgaris* and *Dunaliella tertiolecta*. Arch. Biol. Sci. 65 (4), 1447–1457.
Kramarova, Z., Fargasova, A., Molnarova, M., Bujdos, M., 2012. Arsenic and selenium interactive effect on alga *Desmodesmus quadricauda*. Ecotoxicol. Environ. Saf. 86, 1–6.
Li, W.T., Xu, Z.X., Li, A.M., Wu, W., Zhou, Q., Wang, J.N., 2013. HPLC/HPSEC-FLD with multi-excitation/emission scan for EEM interpretation and dissolved organic matter analysis. Water Res. 47 (3), 1246–1256.
Liang, J., Ning, X.A., Kong, M., Liu, D., Wang, G., Cai, H., et al., 2017. Elimination and ecotoxicity evaluation of phthalic acid esters from textile-dyeing wastewater. Environ. Pollut. 231 (Pt 1), 115–122.
Liang, J., Ning, X.A., Sun, J., Song, J., Lu, J., Cai, H., et al., 2018a. Toxicity evaluation of textile dyeing effluent and its possible relationship with chemical oxygen demand. Ecotoxicol. Environ. Saf. 166, 56–62.
Liang, J.Y., Ning, X.A., Sun, J., Song, J., Hong, Y.X., Cai, H.L., 2018b. An integrated permanganate and ozone process for the treatment of textile dyeing wastewater: efficiency and mechanism. J. Clean. Prod. 204, 12–19.
Liu, H., Weisman, D., Ye, Y.B., Cui, B., Huang, Y.H., Colon-Carmona, A., et al., 2009. An oxidative stress response to polycyclic aromatic hydrocarbon exposure is rapid and complex in Arabidopsis thaliana. Plant Sci. 176 (3), 375–382.
Mecozzi, M., Pietrantonio, E., Pietroletti, M., 2009a. The roles of carbohydrates, proteins and lipids in the process of aggregation of natural marine organic matter investigated by means of 2D correlation spectroscopy applied to infrared spectra. Spectrochim. Acta Mol. Biomol. Spectrosc. 71 (5), 1877–1884.
Mecozzi, M., Pietroletti, M., Gallo, V., Conti, M.E., 2009b. Formation of incubated marine mucilages investigated by FTIR and UV–VIS spectroscopy and supported by two-dimensional correlation analysis. Mar. Chem. 116 (1–4), 18–35.
Meng, Y., Yao, C., Xue, S., Yang, H., 2014. Application of Fourier transform infrared (FT-IR) spectroscopy in determination of microalgal compositions. Bioresour. Technol. 151, 347–354.
Neilen, A.D., Hawker, D.W., O'Brien, K.R., Burford, M.A., 2017. Phytotoxic effects of terrestrial dissolved organic matter on a freshwater cyanobacteria and green algae species is affected by plant source and DOM chemical composition. Chemosphere 184, 969–980.
Nestler, H., Groh, K.J., Schonenberger, R., Behra, R., Schirmer, K., Eggen, R.I., et al., 2012. Multiple-endpoint assay provides a detailed mechanistic view of responses to herbicide exposure in Chlamydomonas reinhardtii. Aquat. Toxicol. 110-111, 214–224.
Ni, L., Rong, S., Gu, G., Hu, L., Wang, P., Li, D., et al., 2018. Inhibitory effect and mechanism of linoleic acid sustained-release microspheres on Microcystis aeruginosa at different growth phases. Chemosphere 212, 654–661.
OECD, 2011. OECD Guideline for the Testing of Chemicals, Alga, Growth Inhibition Test, 201. OECD.
Pandey, S., Rai, R., Rai, L.C., 2012. Proteomics combines morphological, physiological and biochemical attributes to unravel the survival strategy of Anabaena sp. PCC7120 under arsenic stress. J. Proteom. 75 (3), 921–937.
Pazdzior, K., Wrebiak, J., Klepacz-Smolka, A., Gmurek, M., Bilinska, L., Kos, L., et al., 2017. Influence of ozonation and biodegradation on toxicity of industrial textile wastewater. J. Environ. Manag. 195 (Pt 2), 166–173.
Petala, M., Kokokiris, L., Samaras, P., Papadopoulos, A., Zouboulis, A., 2009. Toxicological and ecotoxic impact of secondary and tertiary treated sewage effluents. Water Res. 43 (20), 5063–5074.
Punzi, M., Nilsson, F., Anbalagan, A., Svensson, B.M., Jonsson, K., Mattiasson, B., et al., 2015. Combined anaerobic-ozonation process for treatment of textile wastewater: removal of acute toxicity and mutagenicity. J. Hazard Mater. 292, 52–60.
Ramadass, K., Megharaj, M., Venkateswarlu, K., Naidu, R., 2017. Toxicity of diesel water accommodated fraction toward microalgae, *Pseudokirchneriella subcapitata* and *Chlorella sp. MM3*. Ecotoxicol Environ Saf. 142, 538–543.
Raptis, C.E., Juraske, R., Hellweg, S., 2014. Investigating the relationship between toxicity and organic sum-parameters in kraft mill effluents. Water Res. 66, 180–189.
Richardson, C.E., Hennebelle, M., Otoki, Y., Zamora, D., Yang, J., Hammock, B.D., et al., 2017. Lipidomic Analysis of Oxidized Fatty Acids in Plant and Algae Oils. J. Agric. Food Chem. 65 (9), 1941–1951.
Silva, A., Figueiredo, S.A., Sales, M.G., Delerue-Matos, C., 2009. Ecotoxicity tests using the green algae *Chlorella vulgaris*-a useful tool in hazardous effluents management. J. Hazard Mater. 167 (1-3), 179–185.
Steinberg, C.E.W., Kamara, S., Prokhotskaya, V.Y., Manusadzianas, L., Karasyova, T.A., Timofeyev, M.A., et al., 2006. Dissolved humic substances - ecological driving forces from the individual to the ecosystem level? Freshw. Biol. 51 (7), 1189–1210.
Taibi, K., Taibi, F., Abderrahim, L.A., Ennajah, A., Belkhodja, M., Mulet, J.M., 2016. Effect of salt stress on growth, chlorophyll content, lipid peroxidation and antioxidant defence systems in Phaseolus vulgaris L. South Afr. J. Bot. 105, 306–312.
Tigini, V., Giansanti, P., Mangiavillano, A., Pannocchia, A., Varese, G.C., 2011. Evaluation of toxicity, genotoxicity and environmental risk of simulated textile and tannery

wastewaters with a battery of biotests. Ecotoxicol. Environ. Saf. 74 (4), 866–873.
Wei, Y., Zhu, N., Lavoie, M., Wang, J., Qian, H., Fu, Z., 2014. Copper toxicity to Phaeodactylum tricornutum: a survey of the sensitivity of various toxicity endpoints at the physiological, biochemical, molecular and structural levels. Biometals 27 (3), 527–537.
Xiao, X., Han, Z.-y., Chen, Y.-x., Liang, X.-q., Li, H., Qian, Y.-c., 2011. Optimization of FDA–PI method using flow cytometry to measure metabolic activity of the cyanobacteria, Microcystis aeruginosa. Phys. Chem. Earth, Parts A/B/C 36 (9-11), 424–429.
Yadav, A., Raj, A., Purchase, D., Ferreira, L.F.R., Saratale, G.D., Bharagava, R.N., 2019. Phytotoxicity, cytotoxicity and genotoxicity evaluation of organic and inorganic pollutants rich tannery wastewater from a Common Effluent Treatment Plant (CETP) in Unnao district, India using Vigna radiata and Allium cepa. Chemosphere 224, 324–332.
Yang, Z.K., Ma, Y.H., Zheng, J.W., Yang, W.D., Liu, J.S., Li, H.Y., 2014. Proteomics to reveal metabolic network shifts towards lipid accumulation following nitrogen deprivation in the diatom Phaeodactylum tricornutum. J. Appl. Phycol. 26, 73–82.
Yu, X., Zuo, J., Tang, X., Li, R., Li, Z., Zhang, F., 2014. Toxicity evaluation of pharmaceutical wastewaters using the alga *Scenedesmus obliquus* and the bacterium *Vibrio fischeri*. J. Hazard Mater. 266, 68–74.
Zhang, H., Du, W., Peralta-Videa, J.R., Gardea-Torresdey, J.L., White, J.C., Keller, A., et al., 2018. Metabolomics reveals how cucumber (Cucumis sativus) reprograms metabolites to cope with silver ions and silver nanoparticle-induced oxidative stress. Environ. Sci. Technol. 52 (14), 8016–8026.
Zhang, M., Lu, T., Paerl, H.W., Chen, Y., Zhang, Z., Zhou, Z., et al., 2019. Feedback Regulation between Aquatic Microorganisms and the Bloom-Forming Cyanobacterium Microcystis aeruginosa. Appl. Environ. Microbiol. 85 (21).
Zhang, Y., Sun, Q., Zhou, J., Masunaga, S., Ma, F., 2015. Reduction in toxicity of wastewater from three wastewater treatment plants to alga *(Scenedesmus obliquus)* in northeast China. Ecotoxicol. Environ. Saf. 119, 132–139.